ELSEVIER

Tribology International 32 (1999) 587–596

TRIBOLOGY INTERNATIONAL

www.elsevier.com/locate/triboint



# Fretting corrosion of materials for orthopaedic implants: a study of a metal/polymer contact in an artificial physiological medium

Bruno Tritschler *, Bernard Forest, Jean Rieu

*Département Mécanique des Biomatériaux et Traitements de Surface, Ecole Nationale Supérieure des Mines de Saint-Etienne, 158, Cours Fauriel, 42023 Saint-Etienne Cedex 2, France*

Received 20 May 1999; received in revised form 15 November 1999; accepted 16 November 1999

**Abstract**

The fretting corrosion behaviour of a 316L SS flat against a PMMA counterface has been investigated in an artificial physiological medium. A specific device has been used to visualize the in situ degradation at the contact interface. Simultaneous analysis of the coefficient of friction and free corrosion potential has shown four distinct stages during fretting experiments. An energy-oriented approach to the fretting process was conducted in tandem with measurement of wear. This method has shown a linear progression in the wear volume of the samples as a function of the interfacial energy dissipated during fretting. The presence of chlorides contributes to a considerable acceleration of the degradation of the stainless steel surface. This process was explained by a mechanism related to crevice corrosion activated by friction. 

*Keywords:* Fretting corrosion; Wear; 316L SS; Orthopaedic implants

## 1. Introduction

When two surfaces in contact are subjected to an oscillatory movement of low amplitude, surface deterioration generally appears [1–4]. The phenomena of wear induced by friction over small displacements, often designated by the term *fretting*, can develop in any mechanical device subjected to alternating movements, such as vibrations or oscillations. Examples include bolted assemblies, cables [5], rotors, riveted joints or electrical contacts.

Damage by fretting involves all kinds of materials: metals, ceramics [6] or polymers [7]. The most important consequence is a drastic reduction in the lifetime of mechanical systems, due to jamming of the parts in contact or, in contrast, the appearance of play.

Environmental effects are of overriding importance in the phenomena of fretting. Some corrosive media, such as chlorides, contribute to a considerable acceleration of wear. The processes involved, in which chemical or electrochemical reactions with the environment predominate, are known as *fretting corrosion* [8,9].

The biomedical field is not immune to these phenomena. Thus, the mechanical devices used in orthopaedic surgery are subject to fretting [10,11]. These mechanisms have been used for many years in assemblies such as screw/plate connections [12,13]. In association with this phenomenon, problems of fretting corrosion in total hip joint prostheses have been observed for several years [14–16]. The most frequently employed method for fixation is by cementing the femoral stem into the bone using a polymer cement, poly(methylmethacrylate) (PMMA). Fig. 1 shows the mode of implantation of such prostheses.

Three groups of materials are widely used at present: 316L austenitic stainless steels, cobalt–chromium alloys and Ti–6Al–4V titanium alloys, much used since the 1970s because of their good mechanical properties combined with high biocompatibility [17].

Small movements develop either immediately on implantation or after a few years of service. These small amplitude movements are all the more dangerous for occurring in an environment rich in chlorides. Instances of loosening of the prosthesis can be explained in part by the great difference in elastic modulus between the

* Corresponding author. Tel.: +33-4-77-42-02-51; fax: +33-4-77-42-00-00.

*E-mail address:* tritschl@sms.emse.fr (B. Tritschler).

0301-679X/99/$ - see front matter 
PII: S0301-679X(99)00099-7

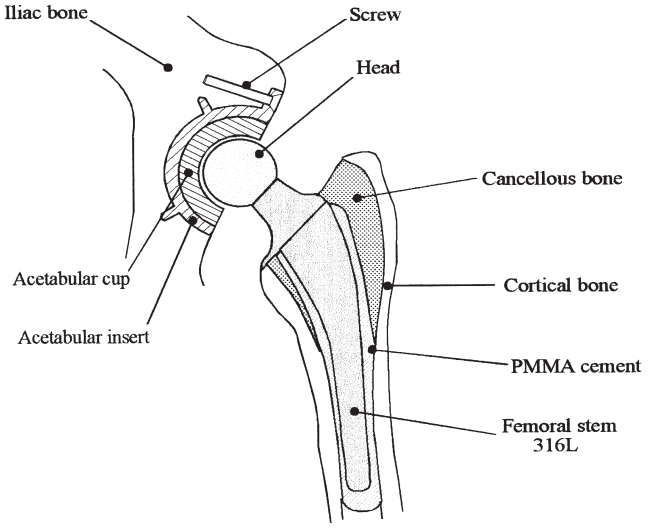


Fig. 1. Diagram showing cemented implantation of a total hip joint prosthesis.

polymer and the metal femoral stem, and in part by imperfect initial fixation resulting from the shape of the prosthesis [18]. Fretting corrosion then causes the formation of debris in the form of a mixture of particles of metallic oxides and polymer. The direct consequences are inflammatory reactions of the surrounding bony tissues and the necessity for a second surgery. Examples are metallosis cases which are due not only to the corrosion of the prosthesis in service, but more likely to the emission and the effects of wear particles produced by fretting [14]. The analysis of prostheses which have been removed does not always reveal the actual reasons for their failure. It was therefore necessary to develop test methods to study the fretting behaviour of materials used for implants. One solution consists in reproducing as faithfully as possible the functioning of a hip joint prosthesis by means of walk simulators. Such devices, based on the average behaviour of the patients, are difficult to use and costly to create. Thus the need to develop techniques of in vitro investigation led to the design of devices capable of producing wear faces similar to those observed on explanted prostheses, by means of simple, rapid and reproducible tests. Many previous studies have indeed examined the problems of deterioration of orthopaedic implants in general: experimental techniques have been created to reproduce it and surface treatments devised to remedy it [19–22]. Confinement appears to be an essential factor in the deterioration. In the case of large amplitude displacements, to which the term "fretting" cannot be applied, the degree of deterioration is observed to vary according to the degree of confinement. Earlier studies were carried out on a pin made of UHMWPE and a disc of 316L SS in an artificial physiological solution. These showed almost no damage to the surface of the metal [21], while slight polishing of the surface of the polymer had occurred. In contrast, when a UHMWPE hip prosthesis cup was fretted against a 316L SS sphere in Ringer's solution, in a configuration similar to the in vivo relationship between the spherical head and the acetabular cup, a phenomenon of crevice corrosion activated by the friction developed at the surface of the metal, and considerable abrasion of the polymer was observed.

The purpose of the present work was to study the phenomena of wear by fretting corrosion of a metal, 316L stainless steel, in contact with a polymer, poly(methylmethacrylate) (PMMA). The tests, performed in an artificial physiological medium using a device for in situ visualization of the contact surface, led to the development of a qualitative and quantitative approach to fretting corrosion.

## 2. Materials and methods

Cylindrical polymer specimens were rubbed against stainless steel flats. Samples of PMMA were taken from cylindrical bars of 20 mm diameter. They took the form of blocks with a rectangular base of 9 mm×15 mm, with one cylindrical surface of radius $R$=10 mm. The PMMA used was optically transparent (Altuglass®). The plane surface opposite the contact interface was polished to enable observation of the polymer/metal interface through the transparent block. PMMA exhibits a glassy transition at $T_g$=399 K and a sub-$T_g$ ('β') transition at $T_\beta$=226 K. At room temperature, it is a hard, brittle material.

The stainless steel used was the 316L SS (Z2CND17-12). It is a high purity steel as regards inclusions and very low in carbon. It was supplied rapid-quenched after hot rolling. Its chemical composition is shown in Table 1. It is in conformity with the standards for manufacture of orthopaedic implants (ISO standard 5832-1).

The metal samples were 10 mm×10 mm×20 mm parallelepipeds. The friction surface was first polished with diamond paste to 1 μm to a roughness of $Ra$=0.03 μm. Before each test, the metal and polymer samples were cleaned for 10 min in ethyl alcohol in an ultrasonic cleaner and then dried in air. The mechanical characteristics of the materials are shown in Table 2.

The fretting tests were conducted on a TRIBOMINES® device installed on a SCHENCK-PSA 10 servo-hydraulic traction–compression machine. The cylindrical sample of PMMA was mounted on a fixed component provided with a conical aperture through which the contact surface can be observed. The plane sample of 316L SS was fixed in a ball joint, enabling the parallelism of the surfaces in contact to be ensured. The length of the cylinder/plane contact was 15 mm. Once adjusted, the ball joint was fixed immobile relative to the hydraulic cylinder by a clamping screw. The whole experimental set-up is shown in Fig. 2.

Table 1
Chemical composition of 316L SS stainless steel (% w/w)

| Cr | Ni | Mo | C | Si | Mn | P | S | Fe |
|---|---|---|---|---|---|---|---|---|
| 17.3 | 13.7 | 2.68 | 0.029 | 0.63 | 1.70 | 0.025 | <0.01 | Bal. |

Table 2
Mechanical properties of the materials used (suppliers' data)

| | Poisson's ratio $\nu$ | Young's modulus $E$ (GPa) | Yield stress $R_c$ (MPa) | Ultimate tensile strength (MPa) |
|---|---|---|---|---|
| PMMA | 0.35 | 3.5 | 30 | 70 |
| 316L SS | 0.3 | 200 | 280 | 640 |

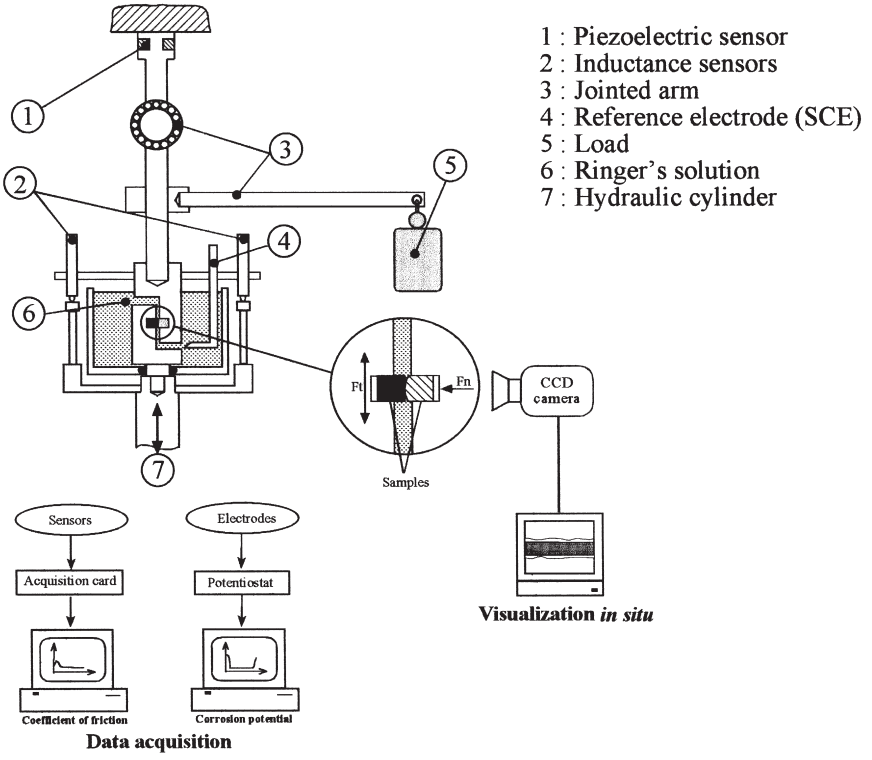


Fig. 2. Tribomines® fretting set-up.

The normal load $F_N$, applied using calibrated masses, lay within the range 0.7–6 N/mm, in order to remain in the elastic domain of the polymer. The displacement amplitude imposed on the metal sample lay within the range ±40 to ±100 μm. The selected cyclical frequency of 1 Hz is comparable to the average walking frequency of the human body. The shape of the cycles is sinusoidal. The movements were monitored in the immediate vicinity of the contact by means of inductance sensors situated on either side of the device. A pre-stressed piezoelectric load-cell was installed on the fixed component in order to measure the tangential force $F_T$. The contact interface between the two samples was displayed on a monitor screen via a CCD camera linked to an optical system. The metal sample was connected to a TACUSSEL PGP 201 potentiostat and a saturated calomel reference electrode (SCE) was placed close to the contact in order to monitor changes in corrosion-free potential during the test. A system of data acquisition and processing was set up to study changes in the coefficient of friction, to record the $F_T$–displacement cycles (or $F_T$–$D$ cycles), and to make electrochemical measurements throughout the test. It must be noted that the shape of the fretting cycles obtained was, for all the tests conducted, characteristic of a gross slip regime within the contact. The fretting tests were performed in a Ringer's solution in

order to simulate human physiological fluids. This solution was prepared in the laboratory to the following formula: NaCl to 8.5 g/l, KCl to 0.25 g/l, $CaCl_2$ to 0.22 g/l, $NaHCO_3$ to 0.15 g/l, with pH value 7.8±0.1. The volume of material removed during the test was evaluated by means of a profilometric technique. After the test, the two metal and polymer samples were carefully cleaned in ethanol in an ultrasonic cleaner in order to remove all traces of debris from the surface. After drying, a TALYSURF profilometer took the profiles at regular intervals across the entire friction surface. The volume of material worn away was then calculated by summing all the elementary volumes thus measured. Calculation by this method provides a more accurate assessment of the volume of abrasion than the weighing method, which would only yield an approximate value due to the small quantities of material worn off by fretting.

The cell containing the stationary Ringer's solution was left open at room temperature in the laboratory atmosphere. Once the samples were placed in the solution and after application of the load, a 30 min wait ensued before the fretting test was started in order to allow the free potential to stabilise.

## 3. Experimental results

### *3.1. Observation and analyses of the surfaces*

The fretting tests carried out in Ringer's solution led to considerable damage to both surfaces. Fig. 3 shows the appearance of the friction zone on the samples, observed using a JEOL-840 scanning electron microscope. In both cases, numerous parallel scratches in the direction of friction are observed. Visual examination of the friction zone on the 316L SS shows deep traces of wear, shiny and scratched in appearance. Around the edge of this zone, a wide orange-red deposit is observed, revealing considerable corrosion phenomena. Fig. 4 shows debris resulting from wear located at the edge of the friction zone at the surface of the 316L SS. Energy dispersion X-ray analyses reveal mainly iron and chromium oxides. The surrounding reddish deposit consists primarily of $Fe_2O_3$ iron oxides.

The PMMA shows an accumulation of fine debris at the limits of the contact, on both sides of the friction zone (Fig. 3). Orange-coloured deposits similar to those observed on the 316L SS sample are also seen all around the friction surface, although in smaller quantities. These are the corrosion products resulting from the electrochemical process occurring on the surface of the metal and little by little transferred onto the surface of the PMMA during the test.

### *3.2. Evolution in coefficient of friction and free corrosion potential*

Four stages were observed in coefficient of friction or free corrosion potential changes during the fretting tests. Fig. 5 shows a typical example of the curves obtained for the tests performed in Ringer's solution. For more clarity, the evolution of both coefficient of friction and free potential were plotted using a logarithmic abscissa.

The first stage, which is very rapid, corresponds to a reduction in the coefficient of friction during the early fretting cycles, associated with a drop in free potential. This initial fall is followed by a slower decrease of the coefficient of friction, while the corrosion potential rises again slightly. The second stage corresponds to an increase in the coefficient of friction associated with a decrease of free potential, though this decrease is less abrupt than that observed at the beginning.

The first few cycles of the test cause the collapse of the layer of oxide initially formed on the surface of the metal, after which strong interaction is observed between the two surfaces now laid bare. This marks the beginning of the damage to the surface of the PMMA and the creation of the first debris which will cover the surface of the metal. Those particles act as a steady-state lubricant film between the counterfaces since the tangential force is applied. This pseudo repassivation causes a new rise in potential with a drop in the coefficient of friction due to the accommodation of the movement by this new

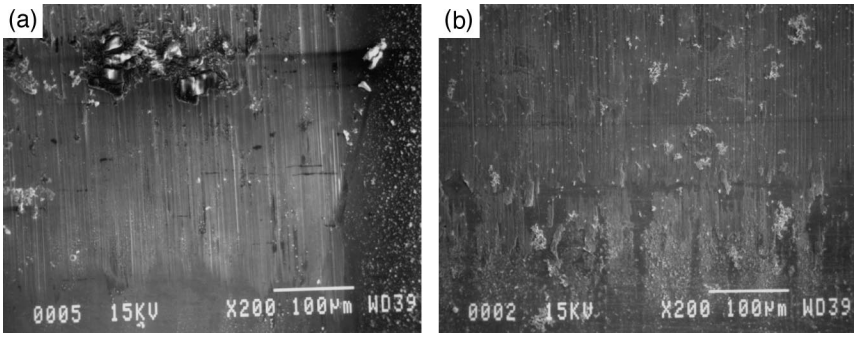


Fig. 3. SEM observation of wear surfaces (frequency 1 Hz, displacement ±40 µm, normal force 4 N/mm, duration of test 20,000 cycles, Ringer's solution). (a) View of surface of 316L SS. (b) View of surface of PMMA.

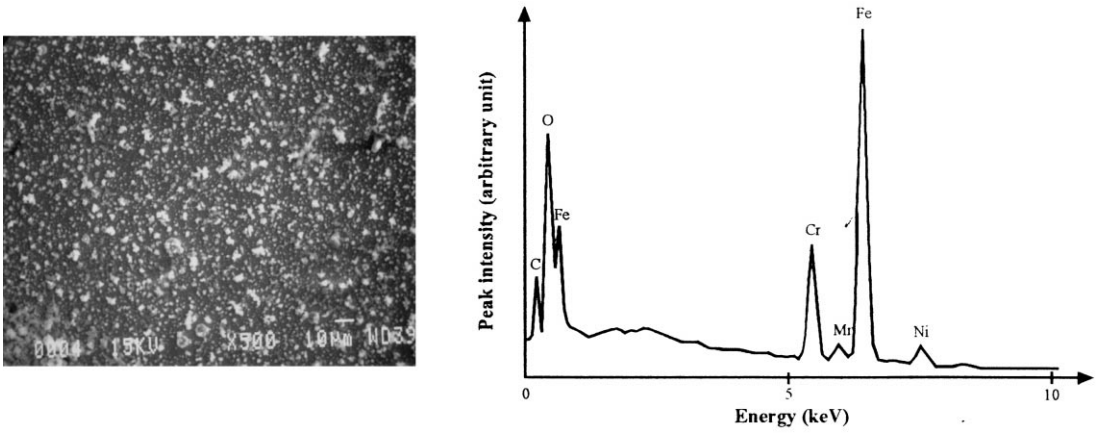


Fig. 4. SEM observation of wear debris on the surface of the 316L SS (frequency 1 Hz, displacement ±40 μm, normal force 4 N/mm, duration of test 20,000 cycles, Ringer's solution). Right: EDX analysis of debris; presence of oxides of iron and chromium.

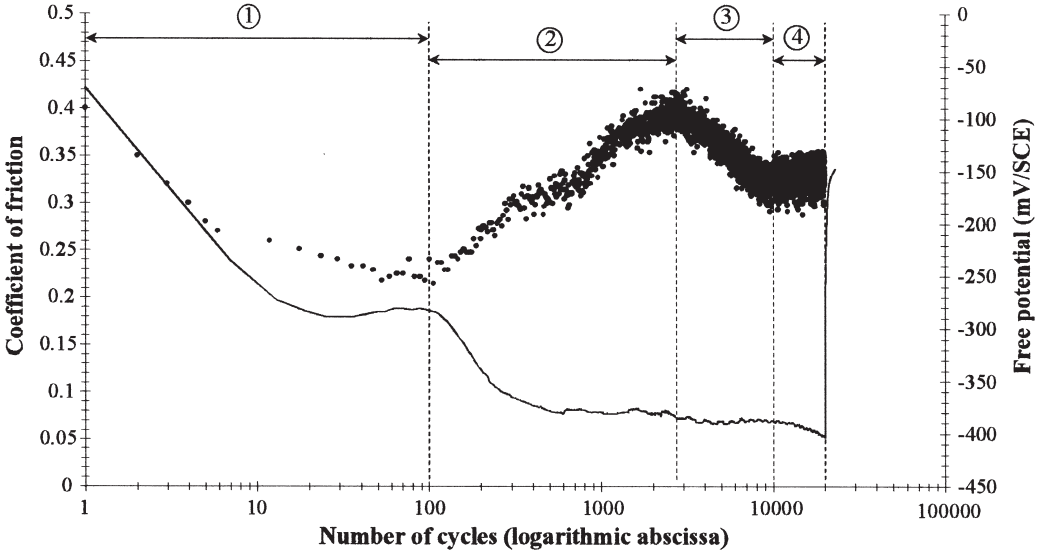


Fig. 5. Coefficient of friction and free corrosion potential as a function of number of cycles. Contact PMMA Ø20/316L SS plane in Ringer's solution. Frequency 1 Hz, displacement ±40 μm, normal force 4 N/mm. 1, breakdown of the oxide layer initially formed and pseudo repassivation; 2, flow of debris—deterioration of the contact interface; 3, degradation of the stainless steel surface; 4, equilibrium in the tribosystem.

freshly formed third body. However, the cleansing action of the surrounding aqueous medium causes the debris to be carried away more or less rapidly to the edge of the friction area. A flow of debris, gradually carried away from the contact surface, builds up. The common damage to the two surfaces results in a regular decrease in corrosion potential to values which are more negative (less "noble")—showing increased electrochemical activity of the stainless steel surface—together with an increase in the coefficient of friction. It is pertinent to remark here that during the first few hundred cycles, any variation in the coefficient of friction is immediately followed by a change in free potential, irrespective of the operating conditions applied. This linked progression of both values has already been shown in previous studies [22].

By in situ observation it is possible to relate the different values measured to the phenomena of deterioration of the polymer/metal interface. Damage to the surfaces is visible from the very first cycles. The consequence of the formation of PMMA debris is the appearance of a white band which adheres to the surface of the metal before gradually disappearing. During the period of rise of the coefficient of friction, increasing deterioration of the contact interface is observed, revealed by the appearance of scars parallel to the direction of movement. An increasing presence of fine, snowy debris at the edge of the contact zone may also be observed.

The third stage of development corresponds to a slow decrease in the coefficient of friction. During this period, the presence in situ of increasingly marked scarring is seen on the surface of the 316L SS, together with the

appearance of small bubbles of gas escaping from the oxidised surface of the metal sample. The free potential gradually stabilises.

The fourth and last stage of development of the coefficient of friction extends through the major part of the test. The tribosystem reaches a condition of stability in which the formation and evacuation of debris, on the one hand, and the phenomenon of corrosion on the other, achieve equilibrium.

Fig. 6 shows how the coefficient of friction is influenced by the normal load applied. Although the process of change mentioned above remains valid, it is nonetheless true that the duration of each stage, at fixed amplitude and frequency, is a function of the normal force applied. The stabilised value of the coefficient of friction diminishes with an increasing applied load. The development of corrosion phenomena causes progressive roughening of the surfaces. It must be supposed, then, that high normal loads (i.e. high contact pressures) encourage "smoothing" of the stainless steel surface by breaking off the irregularities formed by local dissolution phenomena. A priori, a volume of debris proportional to the applied load should be expected, provided all the other parameters remain unchanged.

Fig. 7 shows corrosion-free potential after 10,000 cycles of fretting as a function of applied load. At this stage of the test, variations over time, either of coefficient of friction or of free potential, are minimal. Linear evolution of free potential at 10,000 cycles as a function of applied load is observed. Increasingly negative potential values indicate increasing deterioration of the stainless steel surface. It may be noted that similar results have been obtained in vivo in experiments where metal plates were implanted in sheep [23] walking on a treadmill.

### 3.3. An energy-oriented approach to fretting

The area defined by the $F_T$–$D$ cycle represents the interfacial energy dissipated in the contact during the corresponding fretting cycle [24] (Fig. 8). The whole set of $F_T$–$D$ cycles thus enables definition of the total interfacial energy dissipated during the fretting test by summation of all the elementary interfacial energies corresponding to the area of each cycle. Physically, the total energy dissipated within the tribosystem corresponds to the volume of the 3-D plot (usually known as *friction log*) of the fretting loops as a function of the number of fretting cycles. It contributes to the damage of the surfaces and is dependent on operating conditions: amplitude, normal load and the duration of the test. The graphical representation of the energy dissipated per cycle as a function of time is similar to that of the coefficient of friction (Fig. 9). This similarity is predictable in the case of a gross slip regime—in which the $F_T$–$D$ cycles approximate more closely a quasi-rectangular ideal profile—in that the tangential force is the only variable, the amplitude of slip remaining practically constant throughout all the tests performed.

It was then possible to relate the volume of abraded material to the interfacial energy dissipated during fretting. It should be noted that the energy dissipated by fretting corresponds to two values of wear volumes, one for the PMMA and the other for the 316L SS. Graphical representation of the wear volume as a function of interfacial energy dissipated shows a linear progression

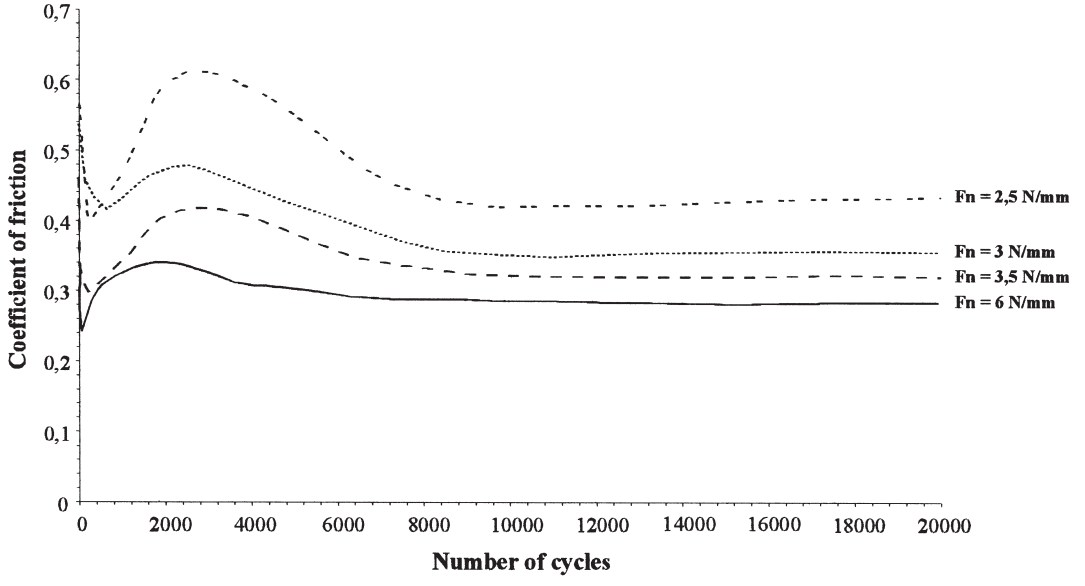


Fig. 6. Coefficient of friction as a function of normal force applied. Contact PMMA Ø20/316L SS plane in Ringer's solution. Frequency, 1 Hz, displacement ±40 μm, 20,000 cycles of fretting.

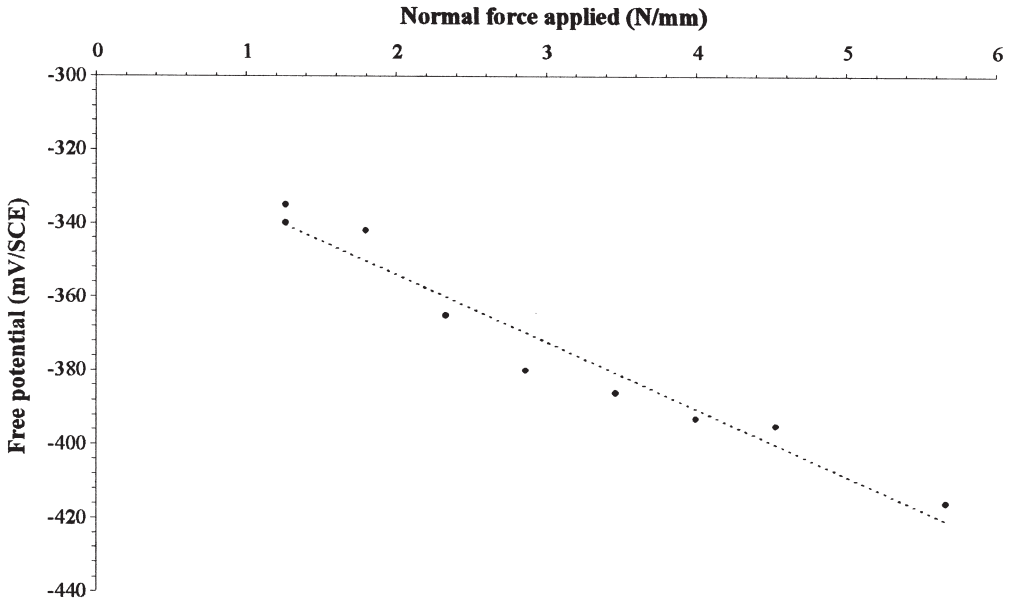


Fig. 7. Free corrosion potential at 10,000 cycles of fretting as a function of normal force applied. Contact PMMA Ø20/316L SS plane in Ringer's solution. Frequency 1 Hz, displacement ±40 μm.

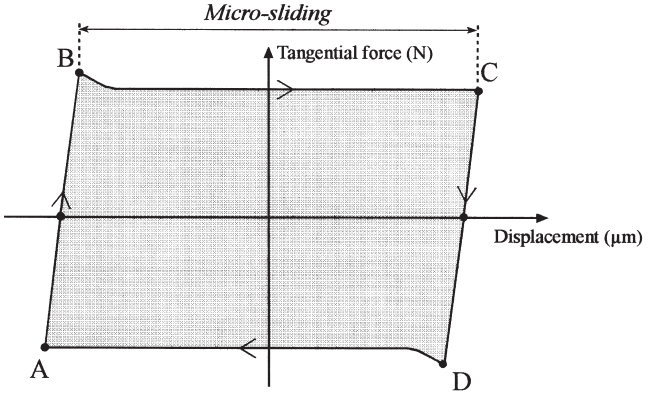


Fig. 8. $F_T$–$D$ cycle used to calculate the interfacial energy dissipated.

(Fig. 10). The volume of PMMA worn away is about five times greater than that of the 316L SS. The loss of material is the principal phenomenon in a full slip regime: the interfacial energy dissipated contributes to the removal of material by the formation of debris followed by its transformation and ejection.

## 4. Discussion

In general, stainless steels such as 316L SS are fairly corrosion resistant due to the formation of a stable oxide film on the surface. The results of this study show that metal/polymer contact subjected to fretting in a chloride-rich solution lead to considerable damage to the surface of the metal. The drop in potential recorded as soon as the movement starts betrays the collapse of the protective oxide film. The continuous fretting action prevents reformation of the film: the potential value remains more or less constant as long as fretting continues. It is only when fretting stops that the potential returns to a more "noble" level, though generally lower than it was at the beginning. Chlorides are known to have a real lubricant effect [5], being responsible, in particular, for reducing adhesion in the contact and for rapid evacuation of the debris. But the presence of chloride ions activates metallic ion exchange: the drop in corrosion potential is evidence of the activation of the stainless steel surface. The small amount of third body persisting at the polymer/metal interface is not enough to ensure adequate protection of the surfaces. There is rapid establishment of a flow of debris, which have a short life in the contact. In this way, wear debris form, but give no protection to the friction surfaces. Fretting corrosion is often taken to be an instance of crevice corrosion activated by the friction. In the present case, the metal/polymer fretting can easily lead to a case of confinement, in that the ratio of imposed displacement/width of contact is low (typically 0.2–0.3) within a full slip configuration. Furthermore, this value diminishes over the period of the test, due to the increase in contact width with the fretting action, which in this way further increases confinement.

Fretting corrosion may be defined as a process of wear in which chemical or electrochemical reactions with the environment predominate. It is then possible to propose an electrochemical mechanism for the degradation of 316L SS subjected to fretting. During friction at free potential on a metal sample, the friction zone behaves as an anode, and the neighbouring surface as a cathode [25,26]. As soon as movement is initiated, rupture of the natural oxide layer exposes the surface of the metal,

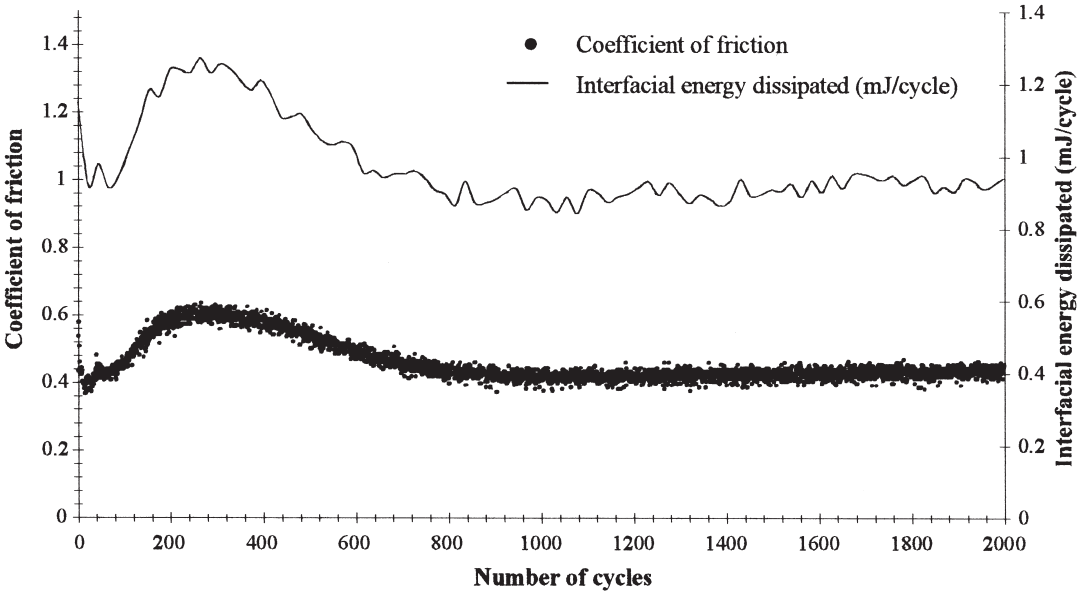


Fig. 9. Combined evolution of coefficient of friction and interfacial energy dissipated per cycle. Contact PMMA Ø20/316L SS plane in Ringer's solution. Frequency 1 Hz, displacement ±40 μm, normal force 1.5 N/mm.

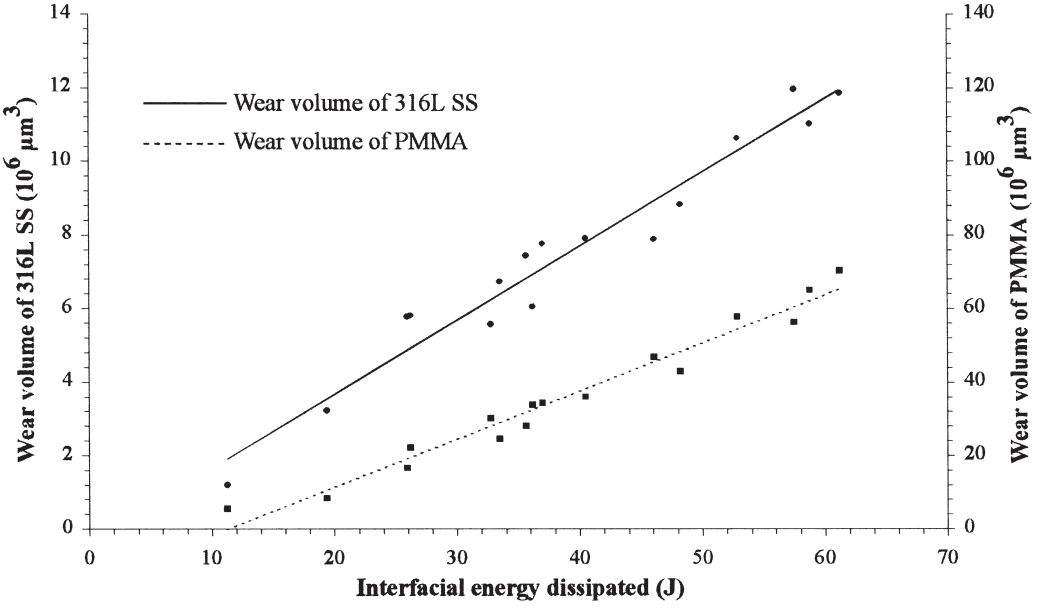


Fig. 10. Wear volume of 316L SS and PMMA as a function of total interfacial energy dissipated in the contact. Tests performed in Ringer's solution.

which is unpassivated and strongly reactive to the oxygen-rich liquid present at the interface. The metal oxidises rapidly and spontaneously, thus reducing the concentration of oxygen in the liquid. The consequence is an increased concentration of free metallic ions at the interface, which occurs after all the oxygen has been used up.

When the limit of solubility of cations is reached, the dissolution is accompanied by the hydrolysis reaction; in the absence of $OH^-$ ions, migration of $Cl^-$ ions occurs in the contact in order to compensate for the formation of $H^+$ ions and ensure the electrical neutrality of the medium:

$$M^{n+} + nH_2O \rightarrow M(OH)_n + nH^+$$

$$nH^+ + nCl^- \rightarrow nHCl$$

Thus the medium becomes locally acidified, leading to accelerated corrosion. This produces, on the external surfaces and in the immediate vicinity of the friction zone, cathodic reactions reducing the oxygen or hydrogen, as follows:

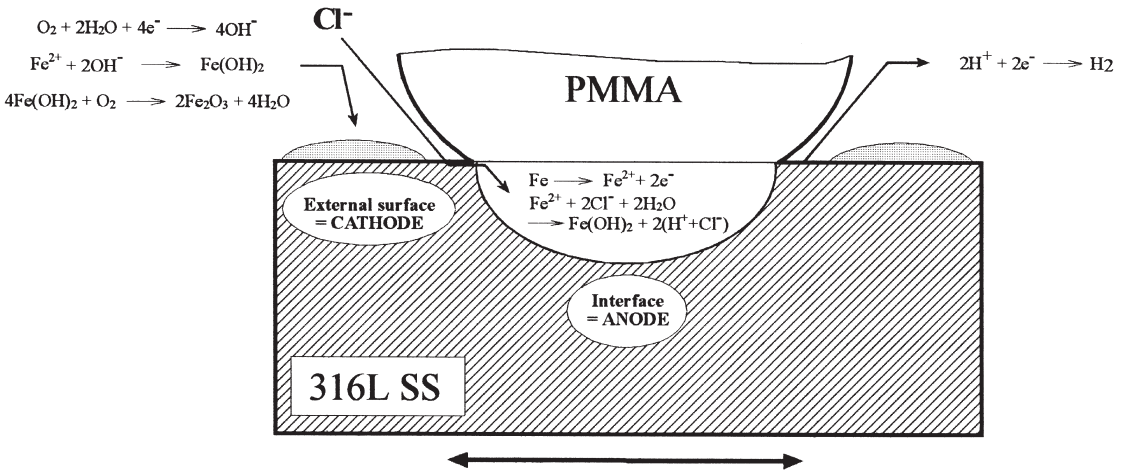


Fig. 11. Electrochemical mechanism responsible for the degradation of the polymer/metal interface in a chloride-rich medium.

$O_2+2H_2O+4e^-\rightarrow 4OH^-$

$2H^++2e^-\rightarrow H_2$

It should be noted that the reduction of hydrogen cannot occur from the thermodynamic point of view until the medium has reached a sufficient level of local acidification. Experimentally, observation showed the formation of gas bubbles, identified as hydrogen, escaping at the edges of the contact zone. The potential from which gas is given off is of the order of $-380\pm10$ mV/ECS. Below that value, small bubbles of gas are formed continuously and escape alternately from each side of the friction interface on the surface of the 316L SS.

The metallic cations which succeed in escaping from the contact may precipitate in the cathodic zone where oxygen reduction occurs. In the case of iron, the reaction chain is as follows:

$O_2+2H_2O+4e^-\rightarrow 4OH^-$

$Fe^{2+}+2OH^-\rightarrow Fe(OH)_2$

$4Fe(OH)_2+O_2\rightarrow 2Fe_2O_3+4H_2O$

The iron oxide $Fe_2O_3$ precipitates in the form of an orange-red deposit in the cathodic zone which surrounds the friction zone. A diagram summarising the whole process of degradation is shown in Fig. 11.

## 5. Conclusion

By the use of the fretting device presented in this study, it has been possible to demonstrate considerable degradation of the stainless steel surface in the case of a PMMA/316L SS contact subjected to fretting in an artificial physiological medium. This degradation is explained by a mechanism related to crevice corrosion activated by friction. In the fretting conditions that we employed, we have been able to demonstrate a linear progression in the wear volume of the samples as a function of the interfacial energy dissipated. This method may be useful for comparing the resistance to fretting of different materials for implants: for a given quantity of energy dissipated, the material showing the lowest wear volume would be, a priori, the material that would best resist this form of wear.

Studies are in progress on the resistance to fretting corrosion of nitrogen stainless steels of type 316LN SS, which displays better resistance to crevice corrosion than 316L SS, and also on cobalt–chromium alloys. Another line of research consists in improving the mechanical characteristics of the surfaces, in particular by nitrogen ion implantation and/or ion nitriding.

## References

[1] Waterhouse RB. Fretting fatigue. Int Mater Rev 1992;37(2):77–97.
[2] Waterhouse RB. Occurrence of fretting in practice and its simulation in the laboratory. In: Material evaluation under fretting conditions. ASTM Special Technical Publication 780. Philadelphia (PA): ASTM, 1982. p. 3–16.
[3] Berthier Y, Vincent L, Godet M. Fretting fatigue and fretting wear. Tribol Int 1989;22(4):235–42.
[4] Godet M. Third bodies in tribology. Wear 1990;136:29–45.
[5] Pearson BR, Brook PA, Waterhouse RB. Fretting in aqueous media, particularly of roping steels in seawater. Wear 1985;106:225–60.
[6] Klaffke D. Fretting wear of ceramics. Tribol Int 1989;22(2):89–101.
[7] Higham PA, Stott FH, Bethune B. Mechanisms of wear of the metal surface during wetting corrosion of steel on polymers. Corrosion Sci 1978;18:3–13.
[8] Waterhouse RB. Fretting corrosion, vol. 10. London: Pergamon Press, 1972.
[9] Waterhouse RB. Fretting in hostile environments. Wear 1975;34:301–9.
[10] Cook SD, Gianoli GJ, Clemow AJ, Haddad RJ. Fretting corrosion in orthopaedic alloys. Biomat Med Dev 1983;11(4):281–92.

[11] Brown SA, Hughes PJ, Merrit K. In vitro studies of fretting corrosion of orthopaedic materials. J Orthop Res 1988;6:572–9.
[12] Thull R, Schaldach M. Corrosion of highly stressed orthopaedic joint replacements. New York/Heidelberg/Berlin: Springer-Verlag, 1976: 242–56.
[13] McKellop HA. Wear in artificial joint materials. Eng Med 1981;3:123–36.
[14] Hoeppner DW, Chandrasekaran V. Fretting in orthopaedic implants: a review. Wear 1994;173:189–97.
[15] Viceconti M, Baleani M, Squarzoni S, Toni A. Fretting wear in modular neck hip prosthesis. J Biomed Mater Res 1997;35:207–16.
[16] Gilbert JL, Buckley CA, Jacobs JJ. In vivo corrosion of modular hip prosthesis components in mixed and similar metal combinations. The effect of crevice, stress, motion and alloy coupling. J Biomed Mater Res 1993;27:1533–44.
[17] Long M, Rack HJ. Titanium alloys in total joint replacement—a materials science perspective. Biomaterials 1998;19:1621–39.
[18] Rose MR, Litsky AS. Biomechanical considerations in the loosening of hip replacement prosthesis. In: Current perspectives on implantable devices. JAI Press Inc, 198. p. 1–45.
[19] Rabbe LM, Rieu J, Lopez A, Combrade P. Fretting deterioration of orthopaedic implant materials. Search for solutions. Clin Mater 1994;15:221–6.
[20] Rieu J, Pichat A, Rabbe LM, Chabrol C, Robelet M. Deterioration mechanisms of joint prostheses materials. Several solutions by ion implantation surface treatments. Biomaterials 1990;11:51–4.
[21] Rieu J, Pichat A, Rabbe LM, Rambert A, Chabrol C, Robelet M. Ion implantation effects on friction and wear of joint prosthesis materials. Biomaterials 1991;12:139–43.
[22] Rabbe LM, Rieu J, Lopez A, Combrade P. Modèle d'étude du fretting corrosion des matériaux utilisés en chirurgie orthopédique. Comportement du couple TA6V-PMMA. Innov Tech Biol Med 1993;14:163–71.
[23] Brown SA, Simpson JP. Crevice and fretting corrosion of stainless steel plates and screws. J Biomed Mater Res 1981;15:867–78.
[24] Fouvry S, Kapsa P, Zahouani H, Vincent L. Wear analysis in fretting of hard coatings through a dissipated energy concept. Wear, 1997;203-204:293–303.
[25] Syrett BC, Wing SS. An electrochemical investigation of fretting corrosion of surgical implant materials. Corrosion-NACE 1978;34(11):379–86.
[26] Sherwin MP, Taylor DE, Waterhouse RB. An electrochemical investigation of fretting corrosion in stainless steel. Corrosion Sci 1971;11:419–29.